Xenopus ADAM 13 is a metalloprotease required for cranial neural crest-cell migration

Dominique Alfandari*‡§, Hélène Cousin*‡§, Alban Gaultier*‡, Katherine Smith†, Judith M. White†, Thierry Darribère* and Douglas W. DeSimone†

Background: Cranial neural-crest (CNC) cells originate from the lateral edge of the anterior neuroepithelium and migrate to form parts of the peripheral nervous system, muscles, cartilage, and bones of the face. Neural crest-cell migration involves the loss of adhesion from the surrounding neuroepithelium and a corresponding increase in cell adhesion to the extracellular matrix (ECM) present in migratory pathways. While proteolytic activity is likely to contribute to the regulation of neural crest-cell adhesion and migration, the role of a neural crest-specific protease in these processes has yet to be demonstrated. We previously showed that CNC cells express ADAM 13, a cell surface metalloprotease/disintegrin. Proteins of this family are known to act in cell-cell adhesion and as sheddases. ADAMs have also been proposed to degrade the ECM, but this has not yet been shown in a physiological context.

Results: Using a tissue transplantation technique, we show that *Xenopus* CNC cells overexpressing wild-type ADAM 13 migrate along the same hyoid, branchial, and mandibular pathways used by normal CNC cells. In contrast, CNC cell grafts that express protease-defective ADAM 13 fail to migrate along the hyoid and branchial pathways. In addition, ectopic expression of wild-type ADAM 13 results in a gain-of-function phenotype in embryos, namely the abnormal positioning of trunk neural-crest cells. We further show that explanted embryonic tissues expressing wild-type, but not protease-defective, ADAM 13 display decreased cell-matrix adhesion. Purified ADAM 13 can cleave fibronectin, and tissue culture cells that express wild-type, but not protease-defective, ADAM 13 can remodel a fibronectin substrate.

Conclusions: Our findings support the hypothesis that the protease activity of ADAM 13 plays a critical role in neural crest-cell migration along defined pathways. We propose that the ADAM 13-dependent modification of ECM and/or other guidance molecules is a key step in the directed migration of the CNC.

Addresses: *Laboratoire de Biologie Moléculaire et Cellulaire du Developpement, Équipe Adhesion et Migration Cellulaires, 9 quai St. Bernard Bat C, 7° etage, Paris 75005, France. †Department of Cell Biology, University of Virginia, Box 800732, School of Medicine, Charlottesville, Virginia 22908, USA.

Present address: ‡Department of Cell Biology, University of Virginia, Box 800732, School of Medicine, Charlottesville, Virginia 22908, USA.

Correspondence: Dominique Alfandari
E-mail: da3s@virginia.edu

§These authors contributed equally to this work.

Received: **15 January 2001**
Revised: **17 April 2001**
Accepted: **30 April 2001**

Published: **26 June 2001**

Current Biology 2001, 11:918–930

0960-9822/01/$ – see front matter

Background

Cranial neural-crest cells (CNC) are critical for the normal morphogenesis of the head and face in that they give rise to bone and cartilaginous elements as well as sensory neurons, glia, connective tissues, and some muscle. Neural crest-cell migration is preceded by an epithelial-mesenchymal transformation, which results in the emigration of neural-crest cells from the neural ectoderm or neural tube. The signals that trigger this transformation and the subsequent directional migration of these cells are unclear, but changes in neural crest-cell adhesion are presumed to play an important part. For example, trunk neural-crest cells have been shown to downregulate N-cadherin expression [1–4] and to increase their affinity for ECM molecules as they begin to migrate [5, 6]. In addition, the segregation of the CNC into well-defined migratory streams in *Xenopus* has recently been reported to involve ephrin signaling, which is likely to provide spatial-boundary information critical for directing CNC cells into the branchial arches [7, 8]. While cell surface-associated protease activity is likely to play a role in regulating CNC adhesive and invasive behaviors, there is no direct evidence linking a neural crest-specific protease in these processes.

ADAMs are proteins that contain a disintegrin and a metalloprotease domain [9]. Of the 31 known ADAMs, 18 are predicted to be active metalloproteases. Two generic functions have been proposed for ADAM proteases: (1)

Figure 1

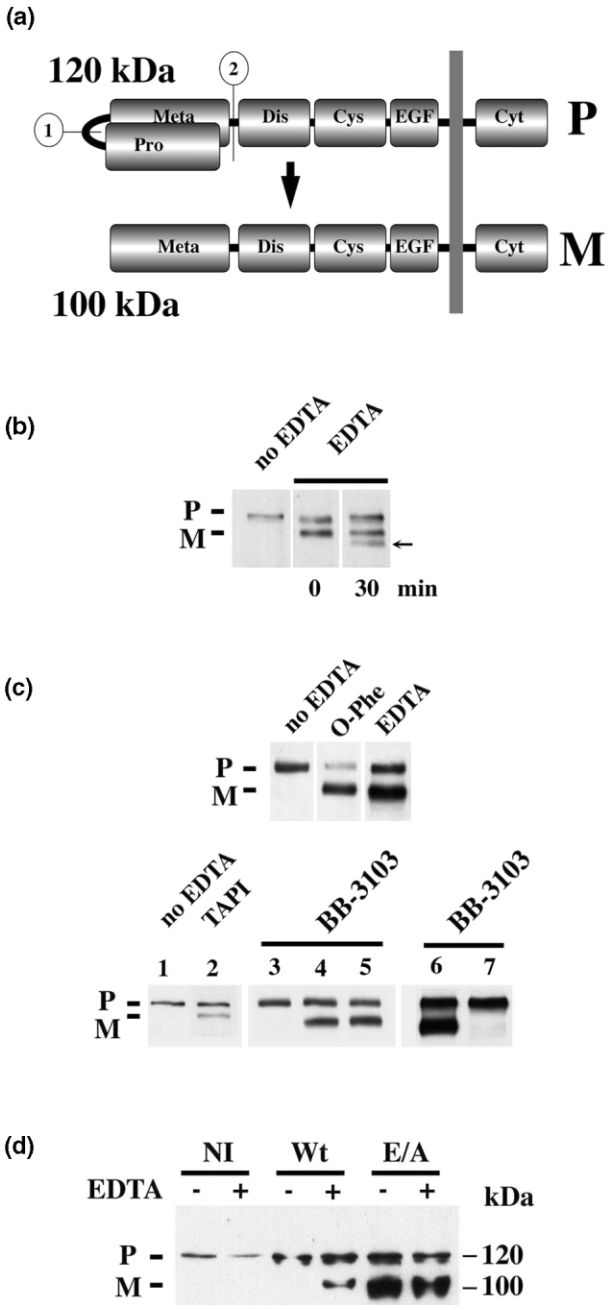

ADAM 13 is a Zn^{2+}-dependent metalloprotease. **(a)** Schematic of the processing of ADAM 13 from its full-length 120 kDa precursor (P) to its 100 kDa metalloprotease-active (M) form (1). The second putative cleavage site between the protease and disintegrin domains is also represented (2). **(b)** Western blot of stage 20 embryos extracted in ESB buffer in the absence (lane 1) or presence (lanes 2–3) of EDTA. Incubation with the 6615F polyclonal antibody (directed against the ADAM 13 cytoplasmic tail) reveals both precursor (P) and metalloprotease-active (M) forms of ADAM 13 after extraction in the presence of 5 mM EDTA (lane 2). A degradation product (arrow) is detected if the EDTA is added 30 min after extraction. **(c)** Western blot of stage 18 embryos expressing Myc-tagged wild-type ADAM 13 detected with the anti-Myc 9E10 mAb. Embryos were extracted in ESB buffer containing, as indicated, either no metalloprotease inhibitor, o-phenanthroline (5 mM), or EDTA (5 mM). Partial protection of the mature ADAM 13 protein is observed with 1 mM TAPI (lane 2). BB-3103 protected ADAM 13 (M) inefficiently at a concentration of 0.05 mM (lane 3), but it fully protected the mature form of the protein at concentrations of 0.5 mM (lane 4) and 5.0 mM (lane 5). mAb 9E10 was used for the immunoprecipitation of Myc-tagged wild-type ADAM 13 from embryo extracts in the presence of 0.5 mM BB-3103. After the sample was washed in extraction buffer containing BB-3103, one half of it was washed in extraction buffer without the inhibitor. After 2 hrs, Laemmli sample buffer was added to both samples, and they were Western blotted with the 9E10 antibody (lanes 6 and 7). Both pro and mature forms of ADAM 13 are visible in the presence of BB-3103 (lane 6), while the mature form is degraded after the removal of BB-3103 (lane 7). **(d)** Western blot of extracts obtained from noninjected embryos (NI) or from embryos expressing either wild-type ADAM 13 or the catalytic-site point mutant (E/A) at stage 18. Embryos were processed as in (b) in the absence (-) or presence (+) of 5 mM EDTA.

local activation of signaling pathways by the shedding of cell surface cytokines and growth factors and (2) cell migration by degradation of the ECM [10, 11]. Although five ADAMs (numbers 9, 10, 12, 17, and 28) have been shown to act as metalloproteases in vitro, the only ADAMs that are known to be catalytically active in vivo are ADAMs 9, 10, and 17, which are all involved in shedding/localized-signaling events. ADAM 9 is responsible for the shedding of HB-EGF from cultured cells [12]. ADAM 10 (*kuzbanian*) acts as a sheddase in the Notch signaling pathway [13–16]. It also appears to function in both axon extension [17] and axon repulsion [18]. ADAM 10 promotes axon repulsion by releasing (shedding) an ephrin [18]. Its role (or that of another ADAM or matrix metalloprotease) in axon extension appears to be as a sheddase that releases the netrin receptor [19]. ADAM 17 (TACE) is involved in multiple ectodomain-shedding events, most notably the release of tumor necrosis factor [20, 21].

Several observations suggest that ADAMs may function in cell migration. First, ADAM 10 and snake venom metalloproteases (SVMPs), the closest ADAM relatives, have been shown to cleave purified ECM components [22, 23] and their receptors [24] in vitro. Second, *Xenopus* ADAM 13 is expressed in cranial neural-crest cells [25], a highly migratory population of cells that gives rise to a variety of tissues, including craniofacial cartilage and the cranial ganglia [26–29]. Third, the secreted ADAM-like gene product, MIG-17, is required for the proper course of distal tip-cell migration in *C. elegans* [30]. Finally, fibroblasts use $\alpha 6\beta 1$ to migrate on a substrate containing the disintegrin domain of ADAM 9 at a more rapid rate than they do on a laminin substrate [31].

While these studies point to the likely involvement of ADAMs in cell migration, there is no direct evidence linking ADAM protease activity with the adhesive and migratory behaviors of a specific cell population in vivo. In this study we show that the metalloprotease activity

of ADAM 13 is required for CNC migration. We also propose that ADAM 13 functions to cleave and remodel fibronectin and possibly other molecules involved in directing CNC migration along defined pathways.

Results and discussion

Xenopus ADAM 13 is a metalloprotease

We previously identified two major forms of ADAM 13 in developing *Xenopus* embryos: a 120 kDa form and a 100 kDa form. By analogy with other ADAMs [32–34], these forms almost certainly represent precursor (P) and presumptive metalloprotease-active (M) forms (Figure 1a) [25]. If tailbud stage embryos were extracted in a buffer containing a nonionic detergent, we observed only the precursor form (Figure 1b). If EDTA was added at the time of extraction, both the precursor and the presumptive metalloprotease-active forms were seen. If EDTA was added 30 min after extraction, degradation products of the presumptive metalloprotease-active form became apparent (Figure 1b, arrow). The presumptive metalloprotease-active form is protected by the metalloprotease inhibitors o-phenanthroline, TAPI [20], and BB-3103 [35]. TAPI and BB-3103 are both hydroxamates that inhibit ADAM and matrix metalloproteases; in this system BB-3103 appears to be more potent (Figure 1c). These data suggest that there is a Zn^{2+}-dependent metalloprotease activity in the embryo extracts that degrades the presumptive metalloprotease-active form of ADAM 13 but leaves intact the Pro form. If ADAM 13 was immunoprecipitated and washed in the presence of 1 mM BB-3103, both forms were retained (Figure 1c, lane 6). If the BB-3103 inhibitor was then washed away from the immunoprecipitate, the mature form disappeared (Figure 1c, lane 7). This shows that the proteolytic activity is directly linked to ADAM 13 and is probably not due to another protease(s) present in the detergent extract.

To test further whether ADAM 13 proteolytic activity is involved in the observed degradation of the M-form (Figure 1b,c), we engineered a point mutation in the active site of the ADAM 13 metalloprotease domain; the catalytic glutamic acid (E) was changed to an alanine (A). Neurula-stage embryos expressing wild-type ADAM 13 and the E-to-A mutant (E/A) were then extracted in nonionic detergent. As seen above with embryos expressing wild-type ADAM 13, the 100 kDa presumptive metalloprotease-active form (M) was only seen if the extracts contained EDTA. With embryos expressing the E/A mutant, however, the 100 kDa mature form was detected whether the embryos were extracted in the presence or absence of EDTA (Figure 1d). This result shows that the E/A mutant does not self degrade in detergent extracts like the wild-type ADAM 13 protein does. Collectively, these findings (Figure 1) indicate that ADAM 13 is a Zn^{2+}-dependent metalloprotease and that substitution of an alanine for the catalytic glutamic acid renders the protease inactive.

Overexpression of ADAM 13 affects neural crest-cell positioning in vivo

ADAM 13 is expressed in *Xenopus* cranial neural-crest cells prior to and during their migration [25]. Cranial neural crest (CNC)-cell migration has been described in detail for this species [36]. During neurulation, CNC cells are located at the lateral edge of the neural plate. They condense to form three segments (mandibular, hyoid, and branchial), each of which migrates as a stream of cells toward the ventral side of the embryo, with the branchial segment further subdividing to yield a total of 4 distinct streams (e.g., see Figure 2k,m).

To identify potential ADAM 13 gain-of-function phenotypes in embryos, we overexpressed the protein by injecting synthetic transcripts encoding Myc-tagged wild-type ADAM 13 into the animal pole of one blastomere at the two-cell stage. These injections resulted in the overexpression of ADAM 13 in CNC and also ectopic expression of the protein in the neural tissue and the surrounding epidermis. The protein was rarely expressed in mesodermal derivatives, and this finding suggests that the mRNA did not diffuse far from the site of injection. The marker *Xslug* [37] was then used for the identification of the cranial and trunk crests at various stages of development. The uninjected side of each embryo (Figure 2) served as a control in each of these experiments. At late gastrula and early neurula stages, no alterations in the pattern of *Xslug* expression were noted (Figure 2b). This indicates that the early formation of the neural crest was unaffected by over-/ectopic expression of ADAM 13. In contrast, at tailbud stages the normally clearly segmented pattern of the CNC into mandibular (m), hyoid (h), and branchial (b) streams (Figure 2e, arrows) was replaced by a single mass of cells adjacent to the neural tube on the injected side (Figure 2d–f, red arrowheads). Ectopic islands of cells expressing *Xslug* were also noted in the trunk region along the entire anterior-posterior axis (Figure 2d,e, blue arrowheads). These displaced cells do not express the CNC-specific marker *Xtwist* [38], and this observation indicates that over-/ectopic expression of ADAM 13 does not respecify trunk crest cells as cranial-crest cells (Figure 2j). Instead, these cells (Figure 2d,e, blue arrowheads) likely represent trunk neural-crest cells that have either emerged prematurely from the neural tube or that have failed to reach the midline because they were released from the neural epithelium during neural-tube closure.

Overexpression in *Xenopus* of ADAM 9 (Dr. Carl Blobel, personal communication) does not appear to affect neural crest-cell development in this manner, as is evidenced by staining for X*slug*. These findings indicate that the neural-crest alterations discussed above are specific to ADAM

Figure 2

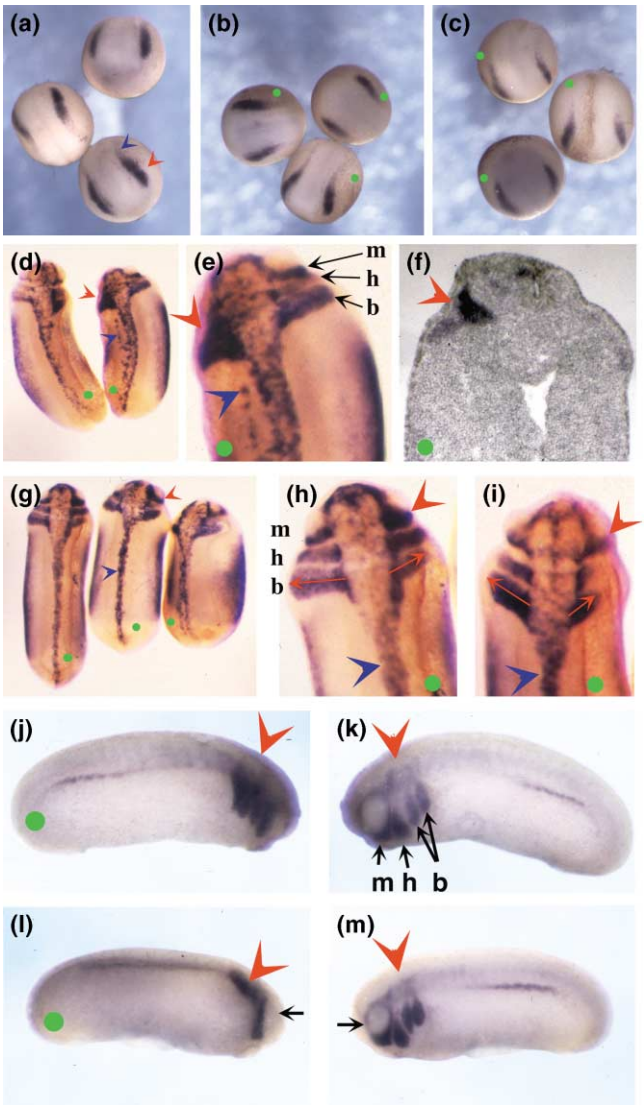

Overexpression of ADAM 13 alters neural crest-cell positioning in vivo. Embryos were injected into the animal pole of one blastomere at the two-cell stage with **(b,d–f,j,k)** 1 ng wild-type ADAM 13, **(c,g,h,l,m)** the E/A point mutant, or **(i)** the E/AΔCyto transcripts. Injected embryos were cultured to **(a–c)** early-neurula stage 13 or (d–m) tailbud stages and processed for (a–i) *Xslug* mRNA expression (blue), (j–m) *Xtwist*, and the Myc-tag epitope (light brown). The green dot indicates the injected side of each embryo; red and blue arrowheads indicate the cranial and trunk crests, respectively. Dorsal views of (a) noninjected control embryos, (b) wild-type embryos, or (c) E/A mutants at stage 13 show no difference in the *Xslug* expression pattern. (d) Dorsal views of wild-type transcript-injected stage 25 (left) and 22 (right) embryos. (e) A higher-magnification view of the stage 22 embryo in (d) shows that the three cranial-crest segments visible on the control side (mandibular, m; hyoid, h; and branchial, b) appear as a single mass on the injected side (red arrowhead). (d,e) Islands of ectopic *Xslug*- positive trunk crest cells (blue arrowheads) are also noted in the flank on the injected side. (f) A horizontal section of a stage 24/25 embryo confirms the location of the cranial crest expressing *Xslug* on the injected side. *Xslug* expression in the head is weak at this stage, as seen in the noninjected control side (e.g., stage 25 embryo on the left in [d]). (g) Dorsal views of tailbud embryos (stage 24, left; stage 22, right) expressing the E/A point mutant. The pattern and position of the trunk crest is normal, although subtle differences in the cranial crest are observed; (h) the extent of migration of cranial crest segments on the injected side is decreased relative to that of the control side (red arrows). (i) Stronger defects are observed in embryos overexpressing the E/AΔCyto protein. (j–m) Lateral views of tailbud stage embryos injected with wild-type ADAM 13 (j,k) or the E/A mutant (l,m). Injected embryos were stained with the cranial neural crest-cell marker *Xtwist*. As seen with *Xslug*, the cranial-crest segments of the embryo injected with wild-type ADAM 13 are not as clearly defined as those in the contra-lateral noninjected side (compare [j] and [k]). Interestingly, overexpression of the E/A ADAM 13 (compare [l] and [m]) has dramatically reduced the migration of cells from the hyoid and branchial crest segments (red arrowhead).

13 and are not likely to be a general consequence of overexpressing any ADAM with an active metalloprotease.

ADAM 13 metalloprotease activity is required for cranial neural crest-cell migration

In contrast to the amalgamated appearance of the cranial crest in embryo halves overexpressing wild-type ADAM 13 (Figure 2d–f, red arrowheads), the three streams of CNC remained well resolved in embryo halves injected with the protease-defective E/A point mutant (Figure 2g,h). In most embryo halves expressing a protease-defective ADAM 13, however, it appeared that there was a reduction in the extent of ventrolateral migration of the CNC streams, particularly of the hyoid and branchial segments (Figure 2h). In addition, ectopic islands of *Xslug*-stained cells were never observed in the trunks of embryo halves that express protease-defective E/A ADAM 13 (Figure 2g,h). This indicates that the observed displacement of the trunk neural-crest cells in wild-type ADAM 13-injected embryos is dependent on ADAM 13 metalloprotease activity. As with wild-type ADAM 13, there were no differences noted in patterns of *Xslug* expression in embryos expressing E/A ADAM 13 at the early neurula stage (Figure 2c).

We determined that embryo-to-embryo variability in the severity of inhibition of cranial-crest migration following E/A ADAM 13 expression was probably due to variable amounts of E/A protein expressed at the cell surface. To increase the expression of this mutant construct at the cell surface, we exploited an observation that deletion of the cytoplasmic tail from ADAM 13 augments its surface expression by approximately 8-fold (data not shown), as has similarly been reported recently for ADAM 12 [39]. Indeed, the injection of synthetic transcripts encoding a protease-defective, cytoplasmic tail-minus version of ADAM 13 (E/A ΔCyto) produced a similar, but reproducibly more pronounced, shortening of cranial neural crest-cell streams, particularly of the hyoid and branchial segments (Figure 2i). Importantly, neither E/A ADAM 13 nor E/A ΔCyto ADAM 13 had any apparent effect on

tissues, including the trunk crest, that do not normally express ADAM 13 (Figure 2g–i). Collectively, the results presented in Figure 2g–i suggest that metalloprotease-defective constructs of ADAM 13 act in a dominant-negative fashion to yield a cranial crest-specific loss-of-function phenotype, the inhibition of CNC-cell migration.

To determine whether the E/A mutant could indeed interfere with wild-type ADAM 13 proteolytic activity, as suggested by both the CNC-cell phenotype (Figure 2) and by published data on ADAM 10 [15], we have used a simple and well-defined gain-of-function phenotype induced by wild-type ADAM 13 overexpression and tested the ability of the E/A mutant to rescue this effect. As previously described [40], ADAM 13 overexpression (0.5 ng) induces cement gland expansion in 29% (n = 78) of injected embryos. This phenotype is directly linked to the metalloprotease activity of ADAM 13 since no embryos injected with the E/A point mutant exhibited expanded cement glands. In contrast, when the same amount of wild-type transcript was coinjected with E/A ADAM 13 (0.5 ng), only 11% (n = 85) of the embryos displayed altered cement glands. This result shows that the E/A mutant can interfere with wild-type ADAM 13 proteolytic activity and further suggests that this mutant can act as a dominant negative. Similar dominant-negative properties were also observed in additional experiments, as described below (see Figure 7).

To test whether over-/ectopic expression of ADAM 13 affects neural crest-cell behavior and not merely the expression pattern of *Xslug*, we repeated the injections of wild-type and E/A ADAM 13 and stained for the CNC-cell marker *Xtwist* [41]. As seen for *Xslug*, in embryos that overexpress wild-type ADAM 13, the three initial CNC segments appear to merge, as is evidenced by staining for *Xtwist* (Figure 2j). In contrast, the uninjected side of the same embryo was not affected (Figure 2k). More significantly, staining of embryos expressing E/A protease-defective ADAM 13 for *Xtwist* revealed a strong retardation in the progression of the hyoid and branchial CNC streams (Figure 2l), and this finding reinforces the proposal that protease-defective forms of ADAM 13 can act in a dominant-negative fashion in CNC cells. Migration of the posterior margin of the manbidular CNC stream did not appear to be affected by E/A ADAM 13 expression, and this finding suggests that an alternate, possibly compensatory, mechanism is able to promote the migration of these particular cells when ADAM 13 function is perturbed.

Effects of ADAM 13 over-/ectopic expression are specific to the neural crest

We interpret the results presented in Figure 2 as evidence that the observed perturbations of CNC cells in embryos expressing ADAM 13 are due to gain-of-function (with wild-type ADAM 13; Figure 2d–f,j) and loss-of-function (with protease-defective ADAM 13; Figure 2g–i,l) effects on an ADAM 13-driven process in neural-crest cells. An alternate possibility is that the observed changes are an indirect consequence of disruptions in general neural patterning or the result of alterations in normal neural crest-cell proliferation and/or specification. We conducted two sets of experiments to consider these possibilities.

First, we stained for the neural markers *Xsox-2* [37, 42] and *N-tubulin*. *Xsox-2* is expressed in the entire central nervous system, while *N-tubulin* is restricted to future neurons. In embryo halves expressing wild-type (Figure 3a,c, black dot) or E/A (Figure 3b, black dot) ADAM

Figure 3

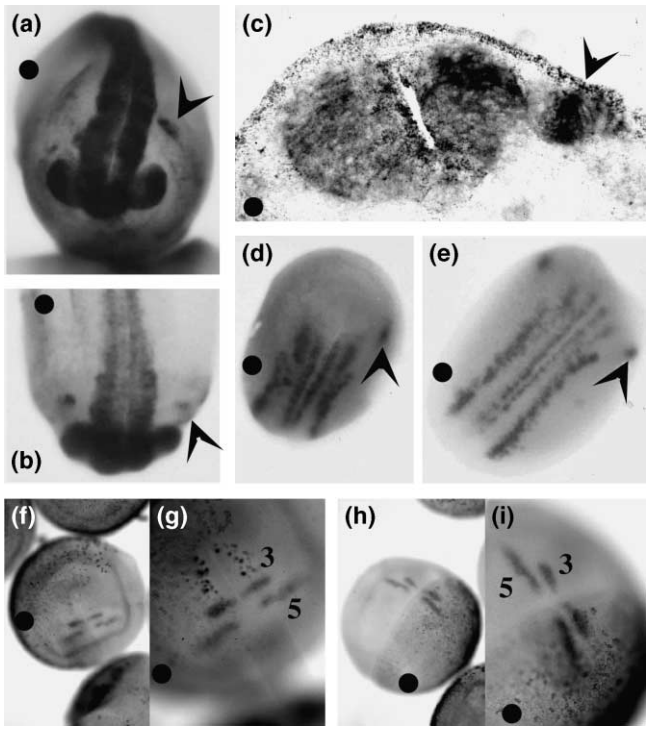

Overexpression of ADAM 13 does not affect central nervous-system formation. Whole-mount in situ hybridization of embryos expressing **(a,c,d)** wild-type ADAM 13 or **(b,e)** the E/A mutant constructs were processed with (a–c) the pan-neural marker *Xsox-2* and (d,e) the neuronal marker *N-tubulin*. Black dots indicate the transcript-injected half of each embryo. Embryos expressing wild-type ADAM 13 lack *Xsox-2*-positive cells in the vicinity of the otic vesicle; (a–c) such cells are present in the E/A and noninjected control halves of each embryo (arrowheads). (c) Transverse section at the level of the putative otic vesicle of an embryo in a stage similar to that in (a). Dorsal views of both (d) wild-type and (e) E/A-expressing embryos at the early-neurula stage (stage 15). (d,e) Lateral expression of *N-tubulin* within the putative trigeminal ganglion (black arrowheads) is absent from (d) the wild-type-injected side. **(f–i)** Dorsal views of neurula-stage (stage 19) embryos overexpressing (f,g) wild-type or (h,i) E/A ADAM 13 and hybridized with the *Xkrox-20* probe. The localization of *Xkrox-20* in rhombomeres 3 and 5 is identical in the uninjected control side compared to the injected side of each embryo.

13, staining for *Xsox-2* was similar to that observed in uninjected control halves, with the exception of a lateral spot of staining at the level of the otic vesicle that was absent in embryo halves injected with wild-type ADAM 13 (Figure 3a,c). This suggests that, aside from the otic placode, neural development appeared normal in ADAM 13 transcript-injected embryos. Similarly, in situ hybridization with *N-tubulin* at the neural plate stage revealed a normal pattern of stripes for primary neurons in embryo halves expressing wild-type (Figure 3d, black dot) or E/A (Figure 3e, black dot) ADAM 13. As observed for *Xsox-2*, a lateral spot of expression (Figure 3d,e, arrowheads, uninjected side) at the level of the trigeminal ganglion [43] was absent in embryo halves injected with wild-type but not E/A ADAM 13 (compare Figure 3d,e, injected sides). The failure of E/A ADAM 13 to affect primary neurogenesis (Figure 3e) is in contrast to the effects reported by Pan and Rubin for a similar mutant of ADAM 10, which when expressed in *Xenopus* leads to increased neurogenesis and expansion of *N-tubulin* staining [15]. We also used the *Xenopus Krox-20* probe to analyze the segmental organization of the hindbrain in embryos overexpressing wild-type and E/A ADAM 13 [44]. In embryos injected with wild-type (Figure 3f,g) or E/A ADAM 13 (Figure 3h,i), *Krox-20* expression in rhombomeres 3 and 5 was at the same anterior-posterior position in the injected versus noninjected sides of each embryo. These results show that the anterior-posterior patterning of the neural tube is not affected by the ectopic expression of wild-type and E/A ADAM 13 proteins.

In a second set of experiments, we tested whether overexpression of wild-type or E/A ADAM 13 affects neural crest-cell proliferation and/or differentiation, which would be reflected in changes in levels of neural crest-cell marker genes. Levels of *Xslug* and *Xtwist* mRNAs in embryos expressing wild-type ADAM 13 or the E/A mutant were quantified by dot blot hybridization at early, mid, and late neurula stages and compared to those of uninjected controls. In these quantitative experiments, no statistically significant differences in the expression of these neural-crest markers were observed (data not shown). These results suggest that the apparent increase in the *Xslug* signal observed with in situ hybridization at the level of the CNC likely represents abnormal positioning rather than an increased number of neural-crest cells.

ADAM 13 function is required for cranial neural crest-cell migration

Based on the results presented in Figures 2 and 3, we conclude that over-/ectopic expression of ADAM 13 constructs primarily affected neural crest-cell migration and not neural-crest growth and/or differentiation. Ectopic expression of wild-type ADAM 13 results in the appearance of trunk neural-crest cells in the lateral pathway, where the migration of these cells is normally restricted. This is consistent with a model in which the normal function of ADAM 13 is to promote neural crest-cell migration. We further propose that overexpression of protease-defective ADAM 13 impedes the normal progression of the CNC cells by interfering with endogenous ADAM 13 metalloprotease activity. These experiments do not allow us to distinguish, however, whether the results observed are due to a direct effect on the migration of neural-crest cells or whether an indirect effect on surrounding tissues leads to a subsequent perturbation of migration pathways. To minimize the possible effects of ADAM 13 (ectopic) expression in surrounding non-CNC tissues, we grafted CNC cells [45] from neurula-stage embryos (stage 18) injected with GFP alone or together with either wild-type or E/A ADAM 13 (donor) into uninjected sibling (host) embryos (Figure 4). Our results show that grafted CNC cells coexpressing GFP with wild-type ADAM 13 migrate toward the ventral side of the embryo with the same timing and in the same segmental pattern (Figure 4a′) as CNC cells expressing GFP alone (data not shown). This suggests that the "fusion" of the CNC segments observed in embryos overexpressing wild-type ADAM 13 (Figure 2d,e) may be due to the ectopic expression (e.g., in the ectoderm) of the protein rather than a function of ADAM 13 overexpression within the CNC cells. In contrast, the migration of CNC cells expressing the E/A ADAM 13 was severely impaired. These cells often remained at the site of initial placement of the graft (Figure 4b′). In some embryos migration was observed in the mandibular segments (Figure 4c′). Whole-mount immunostaining with the 9E10 anti-Myc mAb confirmed that these cells also expressed the Myc-tagged E/A ADAM 13 protein (data not shown). This observation is in accord with previously described experiments in which *Xtwist* staining of the mandibular CNC segment was observed in embryo halves expressing the E/A mutant (Figure 2l).

These data suggest that ADAM 13 metalloprotease function is essential for CNC migration in the hyoid and branchial segments but not for cell migration in the mandibular segment. Time lapse movies of grafted embryos show that fluorescent CNC cells expressing the E/A mutant tend to migrate anteriorly to the mandibular pathway or posteriorly to the vagal pathways rather than enter the hyoid and branchial pathways (example movies may be found at http://faculty.virginia.edu/desimonelab/). These results demonstrate that ADAM 13 metalloprotease function is required by CNC cells to permit their migration through these pathways. Why the migration of CNC cells expressing E/A ADAM 13 is restricted to the mandibular pathway is unclear at present. It may be that migration through the hyoid and branchial arches requires the proteolytic processing of ECM molecules, which otherwise restrict the passage of these cells (see below). Because the developing optic vesicle creates a "bulge" that may serve to physically separate the overlying ectoderm from

Figure 4

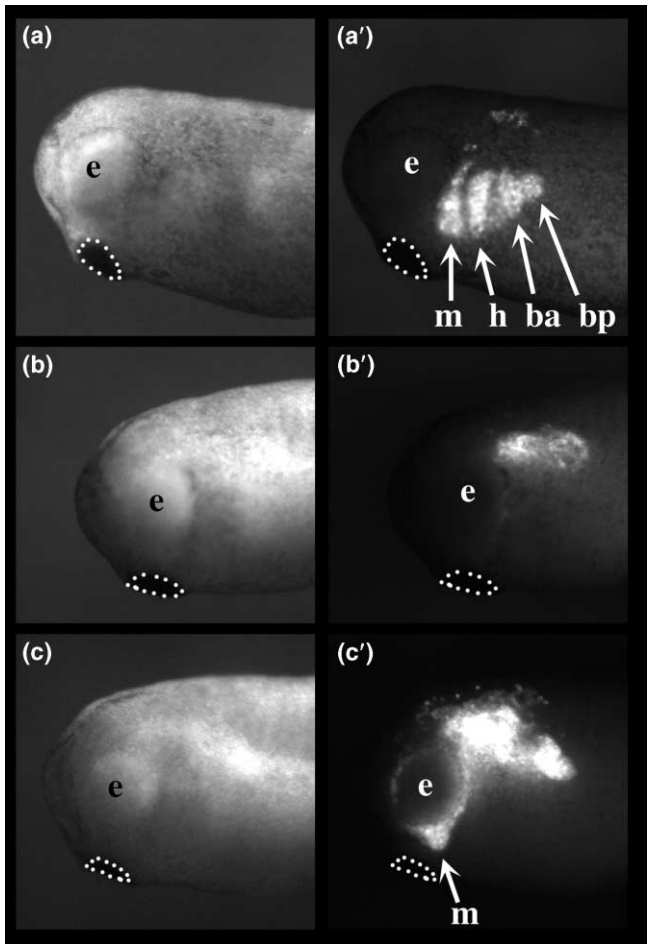

CNC grafts. Transcripts encoding GFP (0.3 ng) alone or in combination with wild-type (0.7 ng) or E/A (0.7 ng) ADAM 13 were injected in one blastomere of two-cell-stage embryos. Labeled cranial neural-crest explants were taken from stage 17–18 *Xenopus* embryos and grafted into unlabeled sibling embryos at the same position (CNC was removed from the host at this position). Lateral views of tailbud stage (stage 24) grafted embryos, with **(a–c)** bright field images on the left and **(a′–c′)** fluorescent images on the right. (a,a′) Embryos that were grafted with cranial-neural crest that expressed both GFP and wild-type ADAM 13 were indistinguishable from (not shown) embryos grafted with CNC expressing GFP alone. (a′) Fluorescent neural-crest cells migrate along pathways normally used by CNC streams (m, mandibular; h, hyoid; ba, branchial anterior; bp, branchial posterior). (b–c) In contrast, cranial neural-crest cells expressing both the E/A ADAM 13 mutant and GFP (b′) do not migrate or (c′) only migrate in the mandibular segment. The cement gland (dotted line) and (e) the future eye are used in each embryo as reference points for the evaluation of neural crest-cell position and the extent of migration.

the underlying mesenchymal tissue in the vicinity of the mandibular stream, it is possible that sufficient "space" is available to permit CNC-cell passage. Alternatively, because the mandibular segment is the first to initiate CNC-cell migration, cells in this segment may not have all been removed from the host embryos prior to receiving the labeled graft. Endogenous ADAM 13-dependent proteolytic activity associated with these wild-type "pioneer" cells may have been sufficient to open the mandibular pathway and may have thus allowed grafted E/A-expressing CNC cells to follow.

ADAM 13 alters cell adhesion on fibronectin

Taken together, the results presented in Figures 2–4 strongly suggest that ADAM 13 plays a critical role in CNC-cell migration in vivo. In order to address how this protein might affect cell migration, we have used two in vitro assays. The first one addresses the adhesion and migration capacity of mesodermal cells expressing ADAM 13 on a fibronectin substrate. These cells were chosen because they do not express detectable levels of ADAM 13 and because they migrate in a predictable fashion under these conditions [46]. Animal caps expressing either wild-type or the protease-defective E/A form of ADAM 13 were dissected from mid-blastula stage embryos and placed on fibronectin substrates in the presence of the mesoderm-inducer activin-A (Figure 5). Under these conditions, non-injected control caps attached to the substrate and underwent convergence-extension movements (Figure 5a). Cells in contact with the substrate at the periphery of the explant sent out lamellapodial extensions and spread and migrated as a cohesive sheet. Animal cap explants expressing wild-type ADAM 13 underwent convergence-extension movements, but cells in contact with the substrate, while remaining adherent, rounded-up, lost contact with their neighbors, and dispersed (Figure 5b,c). This change in behavior was dependent on the metalloprotease activity of ADAM 13. When explants expressing ADAM 13 were cultured in the presence of the metalloprotease inhibitor BB-3103, the number of dispersed and rounded cells as well as the extent of cell dispersion decreased significantly, while adherent cells spread to the same extent as their noninjected counterparts (Figure 5d). In addition, extensive cell rounding and dispersion were rarely observed with animal caps expressing either the E/A point mutant ADAM 13 (Figure 5e,f) or ADAM 10 (H.C. and D.A., unpublished data).

The idea that the ADAM 13 protease can affect cell-adhesive contacts is further suggested by the observation that over-/ectopic expression of wild-type but not E/A ADAM 13 often leads to ectodermal blistering [40], a behavior attributed to decreased contact between the ectoderm and underlying tissue or ECM. Decreased contact between the ectoderm and the underlying tissue [40] may also explain several of the other phenotypes observed following ADAM 13 over-/ectopic expression (Figure 3). For example, both placodal induction and cement gland specification require specific positive and negative signaling between the ectoderm and the underlying tissue [47–49]. ADAM 13 over-/ectopic expression may physically interfere with these signals by decreasing cell-cell

Figure 5

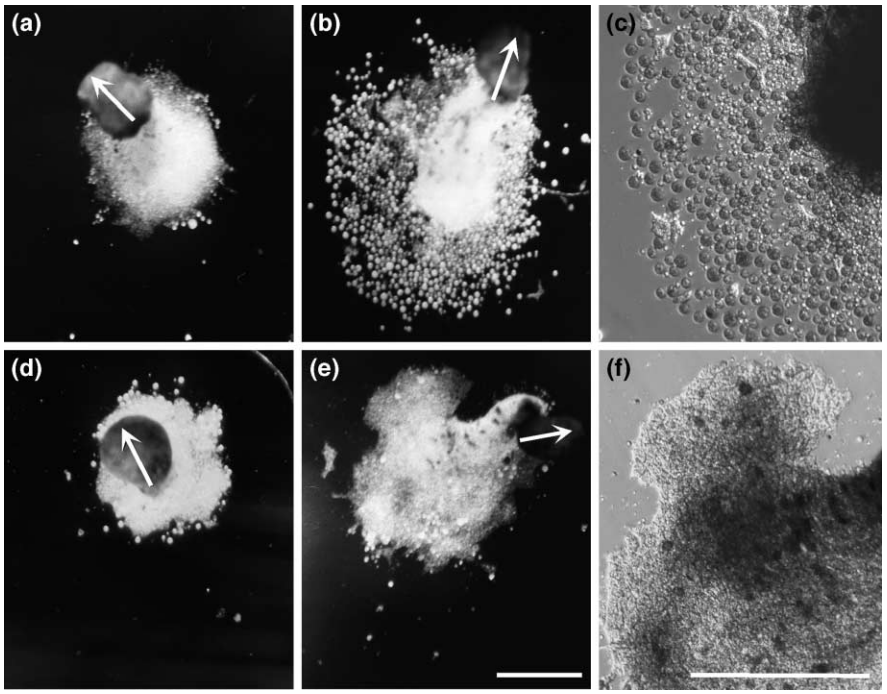

Ectopic expression of ADAM 13 causes perturbation of cell spreading on fibronectin. Animal cap explants expressing **(b–d)** wild-type ADAM 13 or **(e,f)** the protease-defective E/A point mutant were cultured on fibronectin substrates in the presence of 20 U/ml activin-A. **(a)** Under these conditions, noninjected explants undergo convergence extension movements (arrow), while cells in contact with the substrate spread and migrate away from the explant as a cohesive sheet. (b) Explants expressing wild-type ADAM 13 also undergo convergence extension movements (arrow), but (b,c) the cells in contact with the substrate are round and dispersed. These cells remain viable during the course of the assay as determined by trypan blue exclusion (data not shown). (d) Extensive cell spreading occurs in cap cell explants expressing wild-type ADAM 13 in the presence of 0.25 mM BB-3103 protease inhibitor. (e,f) Cell spreading is also observed in animal cap explants expressing the protease-defective E/A mutant construct. (c,f) Higher-magnification views of explants in (b) and (e), respectively. (a,b,d,e, arrows) Converging and extending explant tissue above the plane of focus. The scale bars in (e) and (f) represent 1 mm.

contacts. Interestingly, experimental separation of the outer from the inner ectodermal layer by dissection is sufficient to induce cement gland markers [50]. In our case, ADAM 13 over-/ectopic expression may recapitulate this dissection in vivo at a cellular level. Similarly, ADAM 13 over-/ectopic expression may block a positive signal necessary for the induction of the trigeminal ganglion and the formation of the otic placode [51].

ADAM 13 can remodel a fibronectin substrate and can cleave fibronectin

As indicated by the animal cap results, ADAM 13 overexpression in a migrating population of cells can lead to reduced adhesion to the substrate and rounding-up. This could result either from perturbing cell surface integrins and/or by affecting the ECM. We next asked whether ADAM 13 can modify a fibronectin substrate. We plated *Xenopus* XTC cells transfected with ADAM 13 on a fluorescently labeled fibronectin substrate and observed the cultures after 14 hr by epifluorescence microscopy. Nontransfected XTC cells express low levels of ADAM 13 at their surfaces (Figure 6a and data not shown). Transient transfection with Myc-tagged wild-type or mutant forms of ADAM 13 resulted in expression of additional ADAM 13 protein at the cell surface (Figure 6b and 7b). Wild-type ADAM 13-transfected XTC cells express both the 120 kDa precursor (P) and the 100 kDa metalloprotease-active (M) forms (Figure 7b, left). Biotinylation experiments confirmed that only the 100 kDa metalloprotease-active form of wild-type ADAM 13 is expressed at the cell surface (Figure 7b, right). This is also the case for the E/A point mutant (Figure 7b, right). Nontransfected cells placed on a fluoresceinated fibronectin substrate adhered and spread rapidly (Figure 6a). After 14 hr, the fluorescent substrate was mostly intact (Figure 6a′). In contrast, transfected cells expressing high levels of wild-type ADAM 13 (Figure 6b) modified extensively the fibronectin substrate (Figure 6b′). Alteration of the fibronectin substrate depended on the proteolytic activity of ADAM 13 because transfected cells expressing similar or higher levels of E/A ADAM 13 (Figure 6c and 7b) did not lead to removal of the fibronectin substrate (Figure 6c′) but instead reproducibly demonstrated increased "protection" compared to nontransfected cells (Figure 6a′). In fact, nontransfected XTC cells appreciably remodel the fluorescent fibronectin when left for an additional 10–12 hr (Figure 7a′, arrowheads 1 and 2). Under these conditions XTC cells overexpressing the E/A mutant did not remodel the fibronectin substrate (Figure 7a′, arrowhead 3), and this finding further demonstrates that this protein can inhibit endogenous ADAM 13 function by acting as a dominant negative.

To test whether ADAM 13 can cleave fibronectin directly, we immunoprecipitated fibronectin from *Xenopus* plasma by using the 4H2 mAb [46] and combined it with immunoprecipitated ADAM 13 in the absence (Figure 7c, lane 1) or presence (Figure 7c, lane 2) of the metalloprotease

Figure 6

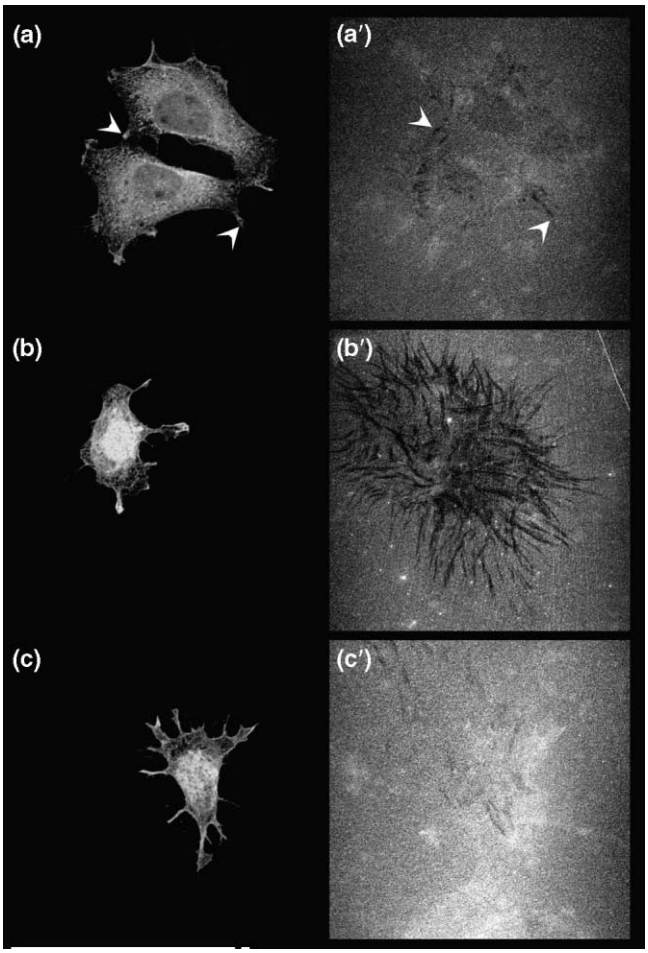

Xenopus XTC cells transfected with wild-type ADAM 13 remodel a fibronectin substrate. *Xenopus* XTC cells were plated on fluorescent fibronectin for 14 hr prior to fixation. Cells were permeabilized and processed for immunofluorescence with a mouse polyclonal antibody directed against **(a)** endogenous *Xenopus* ADAM 13 or **(b–c)** mAb 9E10 directed against the Myc-tag epitope. Fluorescence was observed with a confocal microscope. **(a′–c′)** Fluorescent fibronectin substrates correspond to the same fields as (a–c) immunostained cells. (a) Endogenous ADAM 13 is preferentially localized to the perinuclear endoplasmic reticulum and to cellular extensions at the cell periphery in nontransfected XTC cells (arrowheads). (a′) These cellular extensions colocalize with minor alterations in the fluorescent fibronectin substrate (arrowheads). (b) Cells transfected with wild-type ADAM 13 dramatically modified (b′) the substrate. In contrast, (c′) the fluorescent fibronectin substrate in contact with (c) E/A-transfected cells is comparable to the substrate of (a′) nontransfected control cells.

inhibitor BB-3103. While a large fraction of the fibronectin (220 kDa) remained intact under both conditions (arrowhead a), a fragment recognized by the anti-fibronectin mAb 4H2 was seen in samples in which the protease inhibitor was removed (Figure 7c, lane 1, arrowhead b). Together, these results indicate that ADAM 13 can remodel a fibronectin substrate and can cleave fibronectin at a preferred site.

Figure 7

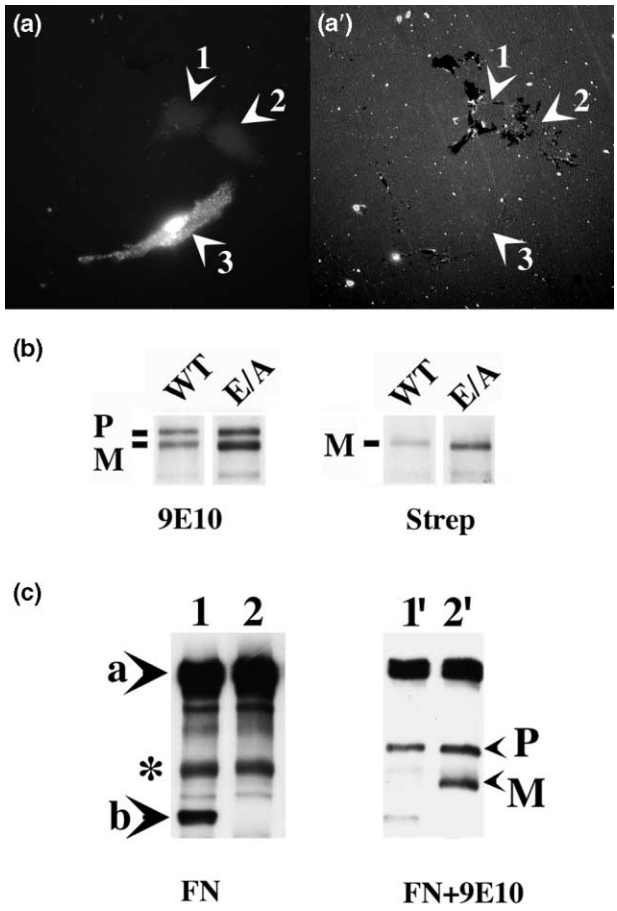

The E/A ADAM 13 inhibits endogenous ADAM 13 remodeling of fibronectin. *Xenopus* XTC cells were plated on fluorescent fibronectin for 24 hr prior to fixation. **(a)** Cells expressing the E/A ADAM 13 were detected with the 9E10 mAb. Fields containing both transfected (arrowhead 3) and nontransfected (arrowheads 1 and 2) cells were selected. The fluorescent fibronectin substrate within the same field is presented in **(a′)**. (a′) During this longer period of incubation (24 hr), nontransfected cells remodeled the substrate (arrowheads 1 and 2), while the cell expressing the E/A ADAM 13 did not (arrowhead 3). **(b)** Surface-biotinylated XTC cells transfected with either wild-type or E/A ADAM 13 were extracted and immunoprecipitated with mAb 9E10. Immunoprecipitated proteins were separated by SDS-PAGE and transferred to nitrocellulose. Blots were either incubated in mAb 9E10 for the detection of total ADAM 13 protein (left panel) or in streptavidin-HRP for the identification of ADAM 13 at the cell surface (right panel). In each case only the mature form (M) of wild-type ADAM 13 or the E/A mutant is present at the cell surface. **(c)** Embryos overexpressing wild-type ADAM 13 were extracted in the presence of BB-3103. Immunoprecipitated wild-type ADAM 13 was incubated with immunoprecipitated fibronectin in the absence (lane 1) or the presence (lane 2) of 0.5 mM BB-3103 for 1 hr at 20°C. The immunoprecipitated fibronectin was analyzed by a Western blot with the 4H2 mAb (left panel). The same blot was then probed with mAb 9E10 for the detection of wild-type ADAM 13 (right panel). The mature (M) form of ADAM 13 is only seen in lane 2′, and this observation confirms the efficiency of the BB-3103 inhibitor in these experiments. The arrowheads in the left panel of (c) point to intact fibronectin (arrowhead a) or the major specific degradation product (arrowhead b, 90 kDa). The asterisk points to a 120 kDa fibronectin fragment, the formation of which is independent of ADAM 13.

Figure 8

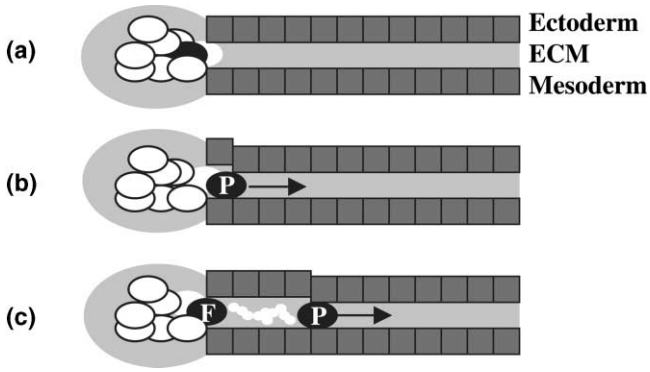

A model for ADAM 13 function in neural crest-cell migration. **(a)** Neural-crest cells (black ovals) are initially part of the neural epithelium. Expression of ADAM 13 at the neural crest-cell surface could help release them from their neighbors and/or the surrounding ECM. **(b)** Following neural crest-cell release, ADAM 13 metalloprotease activity may remodel the ECM that lies between the ectoderm and the underlying mesoderm. This activity may result in the widening of migration pathways. **(c)** While the "**P**ioneer" cells progress through a dense ECM, the "**F**ollower" cells use the open pathways and may respond to directional clues exposed in the "remodeled" matrix.

The ability to remodel a fibronectin substrate is a feature of a number of cultured cells [52–55]. Interestingly, fibronectin remodeling is also increased after transformation by *v-src* [56], and increased levels of pp60Src are associated with matrix remodeling by invadopodia [57, 58]. We have recently reported that the ADAM 13 cytoplasmic domain can bind *Xenopus* Src proteins in vitro [40]. The results presented in the current study show that ADAM 13 is a metalloprotease expressed by a highly invasive population of cells in vivo (i.e., CNC cells) and that ADAM 13 has the ability to remodel a fibronectin substrate when expressed in cultured cells. Together, these results suggest that ADAMs may be involved in the acquisition of invasive properties by tumor cells. Future work will address the possibility that Src proteins stimulate ADAM 13 metalloprotease activity.

A model of ADAM 13 function in cell migration

Proteins of the ADAM family have been shown to act as cell adhesion molecules and, through their metalloprotease domains, as sheddases [10, 11, 59, 60]. It has also been proposed that ADAM metalloproteases may promote cell migration by degrading the ECM. Such an activity has, however, not been demonstrated in a biologically relevant context. Although a more distantly related ADAM-like protein, MIG-17, has recently been shown to be involved in charting the course of cell migration in *C. elegans* [30], a potential target(s) of the putative MIG-17 metalloprotease was not identified. The current study provides evidence that an ADAM is involved in the migration of a highly motile population of cells in vivo and that it may do so by modifying a component of the ECM.

Our results suggest that ADAM 13 may have several specific functions in cranial neural crest-cell migration (Figure 8). First, ADAM 13 may help cells detach from the neuroepithelium by decreasing cell adhesion to the surrounding ECM (Figure 8a). Second, ADAM 13 may cleave proteins of the ECM and thereby open or widen migration pathways (Figure 8b). During their migration, pioneer neural-crest cells may leave directional clues within the remodeled ECM so that following cells may migrate along the same pathways (Figure 8c).

ADAM 13 function in the migrating CNC is likely to involve the cleavage of proteins present in the branchial and hyoid pathways. Our data suggest that these proteins likely include components of the ECM. In this case, the migration of CNC cells expressing the dominant-negative ADAM 13 in the mandibular pathways can be explained either by the absence of the "restrictive" ADAM 13 substrate or by the tissue geometry of this particular region. This apparent requirement for ADAM 13 proteolytic activity in the hyoid and branchial segments but not in the mandibular segment also suggests that ADAM 13 function may help to "direct" CNC migration by unmasking potential guidance cues along their migratory routes. Previous studies in *Xenopus* have shown that proteins from the Ephrin family are involved in restricting the CNC to specific migratory pathways [7, 8]. Future work will investigate the possibility that ADAM 13 is involved in this process, possibly by releasing ephrins, as has been reported for ADAM 10 in axon repulsion [18].

Conclusion

In summary, overexpression of wild-type ADAM 13 and metalloprotease-defective forms of the protein has profound effects on the behavior of neural-crest cells in early *Xenopus* embryos as well as in animal cap explants and XTC cells cultured on fibronectin substrates in vitro. Grafted CNC cells expressing the E/A "dominant-negative" ADAM 13 are restricted from the branchial and hyoid pathways. Our findings are consistent with a model in which the ADAM 13 protease functions in neural crest-cell adhesion and migration. Future work will address the substrate specificity of the ADAM 13 protease, the relative contributions of ADAM 13 metalloprotease activity to matrix remodeling and cell signaling, and the possible roles of other domains of ADAM 13 (e.g., disintegrin domain, cytoplasmic tail) in neural crest-cell biology.

Materials and methods

Egg and embryo preparation

Eggs were obtained from adult *Xenopus laevis*, fertilized, and cultured as described previously [25]. Embryos were staged according to Nieuwkoop and Faber [61].

Transcript preparation and embryo injection

The full-length coding region of *Xenopus* ADAM 13 [25] was cloned into the pCS2 transcription vector [62]. A point mutation substituting an alanine for glutamic acid 341 in ADAM 13 (E/A) was accomplished with the Stratagene Quick Change mutagenesis kit. Both the full-length wild-type and E/A mutant constructs were also tagged with the Myc epitope at their C-termini so that expression could be followed with the 9E10 mAb (Santa Cruz Laboratories). The vector pCS2MycGFP was a generous gift from M. Klymkowsky (University of Colorado, Boulder). It has a single Myc upstream of the GFP and was made by Y. Vourgourakis. All mRNAs were transcribed with SP6 polymerase after linearization of plasmids with Not1 and were prepared for injection as described in [40]. Transcripts (0.5 ng or 1 ng total) were injected close to the animal pole region of one blastomere at the two-cell stage in order for the targeting of ectoderm/neuroectoderm derivatives. The uninjected half of each embryo served as a control in all experiments. In some embryos, the GFP transcript was injected alone as a control for the microinjection procedure.

Characterization of ADAM 13 processing and proteolytic activity

Injected and noninjected control embryos at neurula stages 18 or 20 were solubilized in ESB buffer (100 mM NaCl, 50 mM Tris [pH 7.5], 1% NP40, 2 mM PMSF) either in the presence or absence of 5 mM EDTA. Solubilized glycoproteins were analyzed by Western blotting with the affinity-purified anti-ADAM 13 cytoplasmic-tail antibody (6615F) and ECL detection (Amersham), as described previously [25]. Embryos injected with 1 ng of transcripts encoding Myc-tagged constructs were extracted in the presence of 5 mM EDTA or in the presence of the hydroxamate inhibitors TAPI (kindly provided by Dr. Roy Black at Immunex) or BB-3103 (kindly provided by British Biotech Pharmaceuticals Ltd.). Extracts were processed as above, but after Western blotting they were probed with the 9E10 mAb. Five embryo equivalents per lane of material were analyzed for Western blotting with the 6615F antibody and 1 embryo equivalent per lane with 9E10.

Whole-mount in situ hybridization and immunostaining

Whole-mount in situ hybridization was carried out as described in Harland [63] with slight modification [40]. Staining was performed with BM Purple (Boerhinger-Mannheim) overnight at 20°C. Embryos were also immunostained with the 9E10 anti-Myc antibody (10 μg/ml; Santa Cruz Biotechnology) as described in Hens and DeSimone [64], with secondary anti-mouse HRP conjugated-IgG (5 μg/ml) and DAB staining. Embryos were then cleared in 1% H_2O_2 and 0.5% formamide overnight under strong fluorescent light, dehydrated in 100% methanol, and mounted in benzyl benzoate/benzyl alcohol (2:1 vol/vol). Representative embryos were washed in methanol and embedded in polyethylene glycol 400-distearate (Aldrich), and serial 10 μm sections were cut and mounted in mowiol. Sense transcripts were used in parallel experiments as controls (data not shown). The cDNA templates used for the generation of probes were generously provided by the following investigators: *Xslug* (Roberto Mayor), *Xsox-2* (Robert Grainger), *XCG* (Hazel Sive), *Xkrox-20* (Thomas Lallier). *Xtwist* and *N-tubulin* were obtained by PCR from databank sequences and were cloned with the TOPO-TA cloning kit (Invitrogen).

RNA spot blots

Total RNA from 10 embryos at various stages was extracted as in [65] and precipitated with LiCl. One half embryo equivalent of mRNA was spotted onto nylon membranes with the Spot-Blot System (Schleicher and Schuell) according to the manufacturer's instructions. *Xslug* and *Xtwist* antisense transcripts were labeled with ^{32}P-UTP with the Strip-EZ RNA Probe Synthesis and Removal Kit (Ambion). Blots were prehybridized in 50% formamide, 6× SSPE, 5× Denhardt's solution, 0.5% SDS, and 100 μg/ml sheared salmon sperm DNA for 1–2 hr at 68°C and hybridized with probes for 24 hr at 68°C in the same buffer. Blots were then washed in 1× SSPE/0.5% SDS at room temperature and in 0.1× SSPE/0.1% SDS at 68°C. Spot blots were exposed to a phosphor screen for 24–72 hr and then quantified with ImageQuant software (IQ Mac version 1.2).

Animal cap adhesion/migration assays

Each blastomere at the two-cell stage was injected near the animal pole with 0.5 ng of synthetic transcripts. At the mid-blastula stage, the animal cap regions of injected and noninjected control embryos were dissected and placed on fibronectin substrates (20 μg/ml coating concentration) in the presence of 20 U/ml activin-A (kindly provided by D. Gospodarowicz, Chiron Corporation) diluted in 60% L15 (Gibco/BRL). In some experiments, explants were cultured in the presence of 0.25 mM of the BB-3103 protease inhibitor (British Biotech). Explants were cultured for 18 hr and photographed with a Leica M7Z dissecting scope or by interference contrast with a Leitz (Fluovert FU) inverted microscope.

XTC cell transfection and fibronectin substrate assays

Xenopus XTC cells were grown in 60% L15 supplemented with 10% fetal bovine serum, penicillin (10 IU/ml) and streptomycin (100 μg/ml) (Gibco BRL). Cells were transfected with the Fugene 6 reagent (Boehringer-Mannheim) according to the manufacturer's instructions. Transfected and control cells were grown for 48 hr after transfection, detached with cold CMF (88 mM NaCl, 1 mM KCl, 2.4 mM $NaHCO_3$, 15 mM HEPES [pH 7.6], 1% BSA), and plated on fluorescent fibronectin. Fluorescent substrata were prepared as described in Avnur and Geiger [52], with slight modification. Glass cover slips were coated with 100 μg/ml of bovine FN (Sigma) and fluoresceinated with NHS-Fluoresceine (Sigma) in 50 mM carbonate buffer (pH 9). Cells were left on fluorescent fibronectin for 14 hr in complete culture media, fixed with 4% formaldehyde in 1× MBS, permeabilized with 0.5% Triton X-100 in PBS, and incubated in PBS containing 1% BSA and various antibodies. Secondary anti-mouse IgG linked to Texas red (Molecular Probes) was diluted in PBS/1% BSA at 10 μg/ml. Cells and substrates were imaged with a Leica DMRXE confocal microscope (Leica TCS SP, 488/568 nm).

Cell surface labeling of XTC cells was done with EZ-Link Sulfo-NHS-Biotin (Pierce) in MBS at 1 mg/ml on live adherent cells for 20 min at room temperature. Biotinylated cells were washed with MBS containing 100 mM glycine (pH 7.5) and extracted in TBS, 1% Triton X-100, 2 mM PMSF with 5 mM EDTA. Cellular debris was removed by centrifugation at 13,000 rpm at 4°C for 15 min. Immunoprecipitations were done exactly as described in [66] with the 9E10 monoclonal antibody (SantaCruz Laboratory) linked to Protein-G-agarose (Boehringer Manheim). Biotinylated proteins were detected with HRP-conjugated Streptavidin (Pierce) at 0.2 μg/ml in TBS containing 0.1% Tween-20, followed by ECL treatment as described above.

Cranial neural-crest transplantation

Two cell-stage embryos injected with untagged-GFP (0.3 ng), GFP (0.3 ng) plus wild-type ADAM 13 (0.7 ng), or GFP (0.3 ng) plus E/A ADAM 13 (0.7 ng) were cultured to neurula stages (17–18). Cranial neural-crest cells were transplanted from injected neurulae into uninjected sibling embryos from which a comparable region of cranial neural-crest had been removed (homotopic and homochronic) as described in [45]. Photographs of transplanted embryos (stage 22–25) were taken with a Zeiss dissecting scope equipped for epifluorescence. Immunostaining of the Myc-tagged wild-type and E/A ADAM 13 was performed as described above.

Acknowledgements

H.C. and A.G. are financed by a grant from the Ministère de la Recherche et de la Technologie (97256 and 99750). H.C. was also supported by a post-doctoral fellowship from the Association pour la Recherche contre le Cancer. We would like to thank the Centre National pour la Recherche Scientifique, the Minitère de la Recherche et de la Technologie (ACC SV4), the Association pour la Recherche contre le Cancer (6517), the Ligue Nationale Contre le Cancer, the Fondation pour la Recherche Medicale, and the Institut Universitaire de France for financial support, as well as C. Montmory for technical assistance with tissue sections. We also thank Dr. Mary Kate Worden and Jonna Hamilton for help and advice with statistical analyses.

This work was also supported by grants from the United States Public Health Service (GM48739 [J.M.W.], HD26402 [D.W.D.] and HD01104 [D.W.D.]).

References

1. Duband JL: **Role of adhesion molecules in the genesis of the peripheral nervous system in avians.** *J Physiol* 1990, **84:**88-94.
2. Monier-Gavelle F, Duband JL: **Control of N-cadherin-mediated intercellular adhesion in migrating neural crest cells in vitro.** *J Cell Sci* 1995, **108:**3839-3853.
3. Newgreen DF, Minichiello J: **Control of epitheliomesenchymal transformation. II. Cross-modulation of cell adhesion and cytoskeletal systems in embryonic neural cells.** *Dev Biol* 1996, **176:**300-312.
4. Nakagawa S, Takeichi M: **Neural crest emigration from the neural tube depends on regulated cadherin expression.** *Development* 1998, **125:**2963-2971.
5. Bronner-Fraser M: **Neural crest cell formation and migration in the developing embryo.** *Faseb J* 1994, **8:**699-706.
6. Perris R: **The extracellular matrix in neural crest-cell migration.** *Trends Neurosci* 1997, **20:**23-31.
7. Smith A, Robinson V, Patel K, Wilkinson DG: **The EphA4 and EphB1 receptor tyrosine kinases and ephrin-B2 ligand regulate targeted migration of branchial neural crest cells.** *Curr Biol* 1997, **7:**561-570.
8. Helbling PM, Tran CT, Brandli AW: **Requirement for EphA receptor signaling in the segregation of *Xenopus* third and fourth arch neural crest cells.** *Mech Dev* 1998, **78:**63-79.
9. Wolfsberg TG, Primakoff P, Myles DG, White JM: **ADAM, a novel family of membrane proteins containing A Disintegrin And Metalloprotease domain: multipotential functions in cell-cell and cell-matrix interactions.** *J Cell Biol* 1995, **131:**275-278.
10. Black RA, White JM: **ADAMs: focus on the protease domain**. *Curr Opin Cell Biol* 1998, **10:**654-659.
11. Schlondorff J, Blobel CP: **Metalloprotease-disintegrins: modular proteins capable of promoting cell-cell interactions and triggering signals by protein-ectodomain shedding.** *J Cell Sci* 1999, **112:**3603-3617.
12. Izumi Y, Hirata M, Hasuwa H, Iwamoto R, Umata T, Miyado K, *et al.*: **A metalloprotease-disintegrin, MDC9/meltrin-γ/ADAM 9 and PKCδ are involved in TPA-induced ectodomain shedding of membrane anchored heparin-binding EGF-like growth factor.** *EMBO J* 1998, **17:**7260-7272.
13. Artavanis-Tsakonas S, Rand MD, Lake RJ: **Notch signaling: cell fate control and signal integration in development.** *Science* 1999, **284:**770-776.
14. Blobel CP: **Metalloprotease-disintegrins: links to cell adhesion and cleavage of TNFα and notch.** *Cell* 1997, **90:**589-592.
15. Pan D, Rubin GM: **Kuzbanian controls proteolytic processing of Notch and mediates lateral inhibition during *Drosophila* and vertebrate neurogenesis.** *Cell* 1997, **90:**271-280.
16. Qi H, Rand MD, Wu X, Sestan N, Wang W, Rakic P, *et al.*: **Processing of the Notch ligand Delta by the metalloprotease Kuzbanian**. *Science* 1999, **283:**91-94.
17. Fambrough D, Pan D, Rubin GM, Goodman CS: **The cell surface metalloprotease/disintegrin Kuzbanian is required for axonal extension in *Drosophila*.** *Proc Natl Acad Sci USA* 1996, **93:**13233-13238.
18. Hattori M, Osterfield M, Flanagan JG: **Regulated cleavage of a contact-mediated axon repellent**. *Science* 2000, **289:**1360-1365.
19. Galko MJ, Tessier-Lavigne M: **Function of an axonal chemoattractant modulated by metalloprotease activity.** *Science* 2000, **289:**1365-1367.
20. Black RA, Rauch CT, Kozlosky CJ, Peschon JJ, Slack JL, Wolfson MF, *et al.*: **A metalloproteinase disintegrin that releases tumour-necrosis factor-alpha from cells**. *Nature* 1997, **385:**729-733.
21. Moss ML, Jin SL, Milla ME, Burkhart W, Carter HL, Chen WJ, *et al.*: **Cloning of a disintegrin metalloproteinase that processes precursor tumour-necrosis factor-alpha**. *Nature* 1997, **385:**733-736.
22. Jeon OH, Kim DS: **Molecular cloning and functional characterization of a snake venom metalloprotease.** *Eur J Biochem* 1999, **263:**526-533.
23. Millichip MI, Dallas DJ, Wu E, Dale S, McKie N: **The metallo-disintegrin ADAM 10 (MADM) from bovine kidney has type IV collagenase activity in vitro.** *Biochem Biophys Res Commun* 1998, **245:**594-598.
24. Kamiguti AS, Hay CR, Zuzel M: **Inhibition of collagen-induced platelet aggregation as the result of cleavage of α2β1-integrin by the snake venom metalloproteinase jararhagin.** *Biochem J* 1996, **320:**635-641.
25. Alfandari D, Wolfsberg TG, White JM, DeSimone DW: **ADAM 13: a novel ADAM expressed in somitic mesoderm and neural crest cells during *Xenopus laevis* development.** *Dev Biol* 1997, **182:**314-330.
26. Baker CV, Bronner-Fraser M: **The origins of the neural crest. Part I: embryonic induction.** *Mech Dev* 1997, **69:**3-11.
27. Duband JL, Delannet M, Monier F, Garret S, Desban N: **Modulations of cellular interactions during development of the neural crest: role of growth factors and adhesion molecules.** *Curr Top Microbiol Immunol* 1996, **212:**207-227.
28. Erickson CA, Perris R: **The role of cell-cell and cell-matrix interactions in the morphogenesis of the neural crest.** *Dev Biol* 1993, **159:**60-74.
29. Le Douarin NM, Ziller C, Couly GF: **Patterning of neural crest derivatives in the avian embryo: in vivo and in vitro studies.** *Dev Biol* 1993, **159:**24-49.
30. Nishiwaki K, Hisamoto N, Matsumoto K: **A metalloprotease disintegrin that controls cell migration in *Caenorhabditis elegans*.** *Science* 2000, **288:**2205-2208.
31. Nath D, Slocombe PM, Webster A, Stephens PE, Docherty AJ, Murphy G: **Meltrin γ (ADAM-9) mediates cellular adhesion through α6β1 integrin, leading to a marked induction of fibroblast cell motility.** *J Cell Sci* 2000, **113:**2319-2328.
32. Blobel CP, Myles DG, Primakoff P, White JM: **Proteolytic processing of a protein involved in sperm-egg fusion correlates with the acquisition of fertilization competence.** *J Cell Biol* 1990, **111:**69-78.
33. Roghani M, Becherer JD, Moss ML, Atherton RE, Erdjument-Bromage H, Arribas J, *et al.*: **Metalloprotease-disintegtin MDC9: Intacellular maturation and catalytic activity**. *J Biol Chem* 1999, **274:**3531-3540.
34. Yagami-Hiromasa T, Sato T, Kurisaki T, Kamijo K, Nabeshima Y, Fujisawa-Sehara A: **A metalloprotease-disintegrin participating in myoblast fusion**. *Nature* 1995, **377:**652-656.
35. Middelhoven PJ, Ager A, Roos D, Verhoeven AJ: **Involvement of a metalloprotease in the shedding of human neutrophil FcγRIIIB.** *FEBS Lett* 1997, **414:**14-18.
36. Sadaghiani B, Thiebaud CH: **Neural crest development in the *Xenopus laevis* embryo, studied by interspecific transplantation and scanning electron microscopy.** *Dev Biol* 1987, **124:**91-110.
37. Mayor R, Morgan R, Sargent M: **Induction of the prospective neural crest of *Xenopus***. *Dev Suppl* 1995, **121:**767-777.
38. Hopwood ND, Pluck A, Gurdon JB: **A Xenopus mRNA related to Drosophila twist is expressed in response to induction in the mesoderm and the neural crest.** *Cell* 1989, **59:**893-903.
39. Hougaard S, Loechel F, Xu X, Tajima R, Albrechtsen R, Wewer UM: **Trafficking of human ADAM 12-L: retention in the trans-Golgi network**. *Biochem Biophys Res Commun* 2000, **275:**261-267.
40. Cousin H, Gaultier A, Bleux C, Darribere T, Alfandari D: **PACSIN2 is a regulator of the metalloprotease/disintegrin ADAM13**. *Dev Biol* 2000, **227:**197-210.
41. Linker C, Bronner-Fraser M, Mayor R: **Relationship between gene expression domains of Xsnail, Xslug, and Xtwist and cell movement in the prospective neural crest of *Xenopus*.** *Dev Biol* 2000, **224:**215-225.
42. Mizuseki K, Kishi M, Matsui M, Nakanishi S, Sasai Y: ***Xenopus* Zic-related-1 and Sox-2, two factors induced by chordin, have distinct activities in the initiation of neural induction.** *Development* 1998, **125:**579-587.
43. Sasai Y, De Robertis EM: **Ectodermal patterning in vertebrate embryos**. *Dev Biol* 1997, **182:**5-20.
44. Nieto MA, Bradley LC, Wilkinson DG: **Conserved segmental expression of Krox-20 in the vertebrate hindbrain and its relationship to lineage restriction.** *Development* 1991, **(Suppl):**59-62.
45. Borchers A, Epperlein HH, Wedlich D: **An assay system to study migratory behavior of cranial neural crest cells in *Xenopus*.** *Dev Genes Evol* 2000, **210:**217-222.
46. Ramos JW, DeSimone DW: ***Xenopus* embryonic cell adhesion to fibronectin: position-specific activation of RGD/synergy**

site-dependent migratory behavior at gastrulation. *J Cell Biol* 1996, **134:**227-240.
47. Grainger RM, Henry JJ, Saha MS, Servetnick M: **Recent progress on the mechanisms of embryonic lens formation**. *Eye* 1992, **6:**117-122.
48. Sive H, Bradley L: **A sticky problem: the *Xenopus* cement gland as a paradigm for anteroposterior patterning.** *Dev Dyn* 1996, **205:**265-280.
49. LaBonne C, Bronner-Fraser M: **Neural crest induction in *Xenopus*: evidence for a two-signal model.** *Development* 1998, **125:**2403-2414.
50. Bradley L, Wainstock D, Sive H: **Positive and negative signals modulate formation of the *Xenopus* cement gland.** *Development* 1996, **122:**2739-2750.
51. Baker CV, Bronner-Fraser M: **Vertebrate cranial placodes I. Embryonic induction**. *Dev Biol* 2001, **232:**1-61.
52. Avnur Z, Geiger B: **The removal of extracellular fibronectin from areas of cell-substrate contact.** *Cell* 1981, **25:**121-132.
53. Bowden ET, Barth M, Thomas D, Glazer RI, Mueller SC: **An invasion-related complex of cortactin, paxillin and PKCmu associates with invadopodia at sites of extracellular matrix degradation.** *Oncogene* 1999, **18:**4440-4449.
54. Chen WT, Singer SJ: **Fibronectin is not present in the focal adhesions formed between normal cultured fibroblasts and their substrata.** *Proc Natl Acad Sci USA* 1980, **77:**7318-7322.
55. Kelly T, Mueller SC, Yeh Y, Chen WT: **Invadopodia promote proteolysis of a wide variety of extracellular matrix proteins.** *J Cell Physiol* 1994, **158:**299-308.
56. Chen WT, Olden K, Bernard BA, Chu FF: **Expression of transformation-associated protease(s) that degrade fibronectin at cell contact sites.** *J Cell Biol* 1984, **98:**1546-1555.
57. Chen WT: **Proteolytic activity of specialized surface protrusions formed at rosette contact sites of transformed cells.** *J Exp Zool* 1989, **251:**167-185.
58. Chen WT, Wang JY: **Specialized surface protrusions of invasive cells, invadopodia and lamellipodia, have differential MT1-MMP, MMP-2, and TIMP-2 localization.** *Ann N Y Acad Sci* 1999, **878:**361-371.
59. Primakoff P, Myles DG: **The ADAM gene family: surface proteins with adhesion and protease activity.** *Trends Genet* 2000, **16:**83-87.
60. White JM, Bigler D, Chen M, Wolfsberg TG: **ADAMs**. In: *Cell Adhesion: Frontiers in Molecular Biology* Edited by Beckerle M. Oxford: Oxford University Press; 2001.
61. Nieuwkoop PD, Faber J: *Normal table of Xenopus Laevis (Daudin)*. New York: Garland Publishing; 1994.
62. Turner DL, Weintraub H: **Expression of achaete-scute homolog 3 in *Xenopus* embryos converts ectodermal cells to a neural fate.** *Genes Dev* 1994, **8:**1434-1447.
63. Harland RM: **In situ hybridization: an improved whole-mount method for *Xenopus* embryos.** *Meth Cell Biol* 1991, **36:**685-695.
64. Hens MD, DeSimone DW: **Molecular analysis and developmental expression of the focal adhesion kinase pp125FAK in *Xenopus laevis*.** *Dev Biol* 1995, **170:**274-288.
65. Chomczynski P, Sacchi N: **Single-step method of RNA isolation by acid guanidinium thiocyanate- phenol-chloroform extraction.** *Anal Biochem* 1987, **162:**156-159.
66. Alfandari D, Whittaker CA, DeSimone DW, Darribere T: **Integrin alpha v subunit is expressed on mesodermal cell surfaces during amphibian gastrulation.** *Dev Biol* 1995, **170:**249-261.